

## ORIGINAL ARTICLE

# Study of the physicochemical properties of drugs suitable for administration using a lymphatic drug delivery system

Ryoichi Fukumura<sup>1,2</sup> | Ariunbuyan Sukhbaatar<sup>1,2</sup>  | Radhika Mishra<sup>1,2</sup> |  
Maya Sakamoto<sup>1,2,3</sup> | Shiro Mori<sup>1,2,4</sup> | Tetsuya Kodama<sup>1,2,5</sup> 

<sup>1</sup>Laboratory of Biomedical Engineering for Cancer, Graduate School of Biomedical Engineering, Tohoku University, Sendai, Japan

<sup>2</sup>Biomedical Engineering Cancer Research Center, Graduate School of Biomedical Engineering, Tohoku University, Sendai, Japan

<sup>3</sup>Department of Oral Information and Radiology, Tohoku University Graduate School of Dentistry, Sendai, Japan

<sup>4</sup>Department of Oral and Maxillofacial Surgery, Tohoku University Hospital, Sendai, Japan

<sup>5</sup>Department of Electronic Engineering, Graduate School of Engineering, Tohoku University, Sendai, Japan

## Correspondence

Tetsuya Kodama, Laboratory of Biomedical Engineering for Cancer, Graduate School of Biomedical Engineering, Tohoku University, 4-1 Seiryō, Aoba, Sendai, Miyagi 980-8575, Japan.

Email: kodama@tohoku.ac.jp

## Funding

The study was supported by JSPS KAKENHI grant numbers 20K20161 (AS), 18H03544 (SM), 19K22941 (TK), and 20H00655 (TK).

## Abstract

Lymph node (LN) metastasis is thought to account for 20-30% of deaths from head and neck cancer. The lymphatic drug delivery system (LDDS) is a new technology that enables the injection of drugs into a sentinel LN (SLN) during the early stage of tumor metastasis to treat the SLN and secondary metastatic LNs. However, the optimal physicochemical properties of the solvent used to carry the drug have not been determined. Here, we show that the osmotic pressure and viscosity of the solvent influenced the antitumor effect of cisplatin (CDDP) in a mouse model of LN metastasis. Tumor cells were inoculated into the proper axillary LN (PALN), and the LDDS was used to inject CDDP solution into the subiliac LN (SiLN) to treat the tumor cells in the downstream PALN. CDDP dissolved in saline had no therapeutic effects in the PALN after it was injected into the SiLN using the LDDS or into the tail vein (as a control). However, CDDP solution with an osmotic pressure of ~ 1,900 kPa and a viscosity of ~ 12 mPa·s suppressed tumor growth in the PALN after it was injected into the SiLN using the LDDS. The high osmotic pressure dilated the lymphatic vessels and sinuses to enhance drug flow in the PALN, and the high viscosity increased the retention of CDDP in the PALN. Our results demonstrate that optimizing the osmotic pressure and viscosity of the solvent can enhance the effects of CDDP, and possibly other anticancer drugs, after administration using the LDDS.

## KEYWORDS

cisplatin, lymph node metastasis, lymphatic drug delivery system, osmotic pressure, viscosity

## 1 | INTRODUCTION

Lymph node (LN) metastasis is an extremely important factor that determines the prognosis of many types of cancer. It has been estimated that LN metastasis accounts for 20-30% of all deaths in patients with malignant tumors of the head and neck region.<sup>1,2</sup>

Neck dissection is the main curative treatment for head and neck cancer with LN metastasis. However, LN metastasis remains the main cause of death in elderly and presymptomatic patients for whom surgery is unfeasible or challenging. LNs have a rich vasculature,<sup>3,4</sup> and tumors can grow in LNs by replacing the parenchyma without the induction of tumor neovascularization.<sup>5,6</sup>

**Abbreviations:** CDDP, cisplatin; CT, computed tomography; HE, hematoxylin-eosin; HF-US, high-frequency ultrasound system; ICG, indocyanine green; LDDS, lymphatic drug delivery system; LN, lymph node; PALN, proper axillary lymph node; SEM, standard error of the mean; SiLN, subiliac lymph node; SLN, sentinel lymph node; VEGF, vascular endothelial growth factor.

This is an open access article under the terms of the Creative Commons Attribution-NonCommercial License, which permits use, distribution and reproduction in any medium, provided the original work is properly cited and is not used for commercial purposes.

© 2021 The Authors. *Cancer Science* published by John Wiley & Sons Australia, Ltd on behalf of Japanese Cancer Association.

This proliferative process generates focal perfusion defects that are detectable by contrast-enhanced techniques such as ultrasound and computed tomography (CT).<sup>7,8</sup> As tumor growth in a LN is not associated with tumor neovascularization and leads to a loss of blood vessels, it is likely that small-molecule drugs or high-molecular-weight drugs reliant on the enhanced permeability and retention effect<sup>5,9</sup> would not be effective treatments for lymphatic metastases when administered via the vascular system. Additionally, low-molecular-weight anticancer agents administered via the blood circulation have low selectivity for the lymphatic system and thus limited efficacy.<sup>10,11</sup>

LN metastasis develops when cells from the primary tumor enter the surrounding tissues and lymphatic network (including new lymph vessels formed by lymphangiogenesis) to be carried by lymphatic flow to the sentinel LN (SLN).<sup>12</sup> LNs and lymph vessels form a lymphatic network, and tumor cells migrate from upstream LNs to downstream LNs due to unidirectional lymphatic flow. LNs with early-stage micrometastases are difficult to detect using current clinical imaging modalities. Furthermore, treatments for LN metastasis should target not only the SLN but also downstream LNs that may or may not contain metastases. When cervical LN metastasis is detected in patients with head and neck cancer, the metastases are often found only in a few regional LNs around the primary tumor, and the regional LNs connected to the SLN by the lymphatic network are targeted for treatment. We have proposed the theory of LN-mediated hematogenous metastasis,<sup>4,13,14</sup> which states that SLNs can be the starting point of distant metastasis. Based on this theory, we have been developing a lymphatic drug delivery system (LDDS) to treat early-stage LN metastasis that is not detectable by clinical imaging modalities.<sup>7,15,16</sup> The LDDS can be used to inject anticancer drugs directly into the SLNs during the early stage of metastasis, which would deliver the drugs to downstream LNs via the lymphatic vessels and thereby prevent the development of distant metastasis. The dose of drug required for the LDDS is 1000-10,000 times less than that needed for systemic chemotherapy, which greatly reduces the risks of serious side effects (other than drug allergy) that often limit the duration of systemic chemotherapy. However, histopathological analyses have revealed that proliferating tumor cells embolize in the lymph sinuses to inhibit drug delivery into the LN, and solving this problem remains a pivotal issue.<sup>16</sup> In our recent study of the LDDS, we found that changing the osmotic pressure and viscosity of the drug solvent caused the lymphatic sinuses to expand, which allowed the anticancer drug to be delivered around the tumor cells that had embolized in the lymphatic sinuses.<sup>17</sup>

The aim of the present study was to optimize the osmotic pressure and viscosity of the drug solvent so as to maximize the treatment effects of an anticancer drug on tumor cells in the lymphatic sinus of a metastatic LN. Experiments were performed in a mouse model of LN metastasis, and the LDDS was used to administer the drug to an upstream normal LN so that it flowed to the downstream tumor-containing LN via the lymphatic network.

## 2 | MATERIALS AND METHODS

### 2.1 | Solutions

The osmotic pressure of the injected solutions was set between 588 kPa and 3,000 kPa, and the viscosity was set between 1 mPa·s and 55 mPa·s.<sup>17</sup> The osmotic pressure of human serum is 670-706 kPa (275-290 mOsm/kg, where 1 mOsm/kg = 2436 kPa),<sup>18</sup> so the solutions used in the experiments had osmotic pressures that were 0.9-4 times that of serum. The viscosity of plasma is about 1.8 mPa·s at 37°C. Five solutions (I, II, III, IV, and V) were prepared using glucose or polysorbate 80 to adjust the osmotic pressure and viscosity to the required values (Table 1). Solutions I and II consisted of 50% glucose (Otsuka Pharmaceutical), distilled water, and ultrasound contrast agent (Sonazoid; Daiichi-Sankyo) and were used for intranodal lymphangiography of the proper axillary LN (PALN) using a high-frequency ultrasound (HF-US) imaging system (VEVO770; Fujifilm VisualSonics). Glucose was used to maintain the shape of the Sonazoid lipid membrane. Solutions III, IV, and V consisted of polysorbate 80 (NOF), saline solution (Otsuka Pharmaceutical), ethanol, distilled water, and indocyanine green (ICG, 100 µg/mL, Daiichi-Sankyo) with and without cisplatin (CDDP; Fujifilm Wako Pure Chemical) of 1 mg/kg. The osmotic pressure,  $\Pi$ , was calculated by adjusting the molar concentrations of the components according to Van't Hoff's law. The viscosity,  $\mu$ , of each solution was measured at room temperature (25.6-25.8°C) using two tuning fork vibration viscometers (SV-1H and SV-1A; A & D). The Sonazoid particle size distribution was measured using a zeta potential and particle size measurement system (ELSZ; Otsuka Electronics). There were two peaks in the size distributions of solutions I ( $0.8 \pm 0.2 \mu\text{m}$  and  $8.2 \pm 1.4 \mu\text{m}$ ) and II ( $1.0 \pm 0.2 \mu\text{m}$  and  $8.2 \pm 1.4 \mu\text{m}$ ).

**TABLE 1** Solutions used for injection

Solvent physicochemical properties	Glucose		Polysorbate 80		
	I	II	III	IV	V
Osmotic pressure, $\Pi$ (kPa)	588	3,000	588	1,897	2,768
Viscosity, $\mu$ (mPa·s)	1	1	1	12	55
Sonazoid size ( $\mu\text{m}$ )	A	$0.8 \pm 0.2$	$1.0 \pm 0.2$		
	B	$8.2 \pm 1.4$	$8.2 \pm 1.4$		

Five solutions were prepared. Solutions I and II contained glucose as an essential component and consisted of glucose, distilled water, and Sonazoid (used for high-frequency ultrasound imaging of the proper axillary lymph node [PALN]). There were two peaks in the size distribution of A and B. Solutions III, IV, and V contained polysorbate 80 as an essential component and consisted of polysorbate 80, ethanol, saline, distilled water, and indocyanine green (100 µg/mL) with or without cisplatin (CDDP) (1 mg/kg).

## 2.2 | Cells

We used mouse breast cancer FM3A-Luc cells, which express luciferase,<sup>19</sup> vascular endothelial growth factor-A (VEGF-A), and VEGF-B.<sup>20</sup> The cell culture medium consisted of RPMI-1640 (Sigma-Aldrich), 10% (v/v) fetal bovine serum (HyClone), 1% (v/v) L-glutamine-penicillin-streptomycin (Sigma-Aldrich), and 0.5 mg/mL G 418 (Sigma-Aldrich). Cells were cultured at 37°C in 5% CO<sub>2</sub>. The medium was changed every 4-5 days, and the cells were passaged three times before use in experiments.

## 2.3 | Mice

The experiments were carried out in accordance with ethical guidelines and approved by the Institutional Animal Care and Use Committee of Tohoku University. MXH10/Mo-lpr/lpr (MXH10/Mo/lpr) mice (16-19 weeks of age),<sup>19</sup> a congenic strain of MRL/Mp-lpr/lpr and C3H/HeJ-lpr/lpr mice, were bred under specific pathogen-free conditions in the Animal Research Institute, Graduate School of Medicine, Tohoku University, Sendai, Japan. Mice were anesthetized with 2% isoflurane (Abbott Japan Co., Ltd.) using an inhalation gas anesthesia system for small laboratory animals to minimize distress or pain. The anatomical locations and nomenclatures of murine LNs have often been ignored or assigned incorrectly; here, we use the term "subiliac LN" (SiLN) instead of "inguinal LN".<sup>19,21</sup>

## 2.4 | Intrnodal lymphangiography of the PALN using a contrast-enhanced HF-US imaging system

Solution I ( $n = 2$ ) or II ( $n = 2$ ) was injected into the SiLN at a constant rate of 20  $\mu$ L/min (total volume, 400  $\mu$ L) to deliver it to the PALN. The HF-US imaging system (VEVO770 with an RMV-710B transducer; Fujifilm VisualSonics)<sup>22,23</sup> was used to record two-dimensional and three-dimensional images of the PALN in contrast mode at 3-minute intervals for 30 minutes from the start of injection.<sup>8,24,25</sup>

## 2.5 | Tumor inoculation into the PALN

After confirming that the cells were not infected with *Mycoplasma* (mycoplasma detection kit; Lonza Group), the cell suspension was first adjusted to  $1.2 \times 10^6$  cells/mL using phosphate-buffered saline (PBS, Sigma-Aldrich) and then further diluted threefold with 400 mg/mL Matrigel (Collaborative Biomedical Products) to a final concentration of  $4.0 \times 10^5$  cells/mL. The cell suspension was inoculated with a 27G needle. Each mouse was placed under general anesthesia, the skin over the right PALN was incised to expose the LN, and 40  $\mu$ L of FM3A-Luc cell suspension was administered directly into the PALN by bolus injection. The needle was kept in the PALN

for 1 minute to allow the Matrigel to solidify and then removed with 180° rotation of the syringe. The LN surface was washed with saline, and the skin was sutured to minimize cell leakage and cell proliferation. The inoculation day was defined as day 0.

## 2.6 | Administration of CDDP with the LDDS

CDDP (or control solution) was administered with the LDDS on day 7 after tumor cell inoculation (defined as day 0<sup>T</sup>). Solution III, IV, or V with or without CDDP (Table 1) was injected into the right SiLN at a constant rate of 10  $\mu$ L/min (total volume, 200  $\mu$ L) using a syringe pump (Legato100; KD Scientific), previously described by Fujii et al (2018).<sup>26</sup>

Solution III with CDDP was administered into the tail vein (bolus injection) as a control experiment. Luciferase activity (used as an indicator of tumor growth) was measured on days 0<sup>T</sup> (before and after drug injection), 3<sup>T</sup>, 6<sup>T</sup>, and 9<sup>T</sup> using a bioluminescence imaging system (IVIS Lumina LT Series III; PerkinElmer). The SiLN and PALN were imaged on days -7<sup>T</sup>, 0<sup>T</sup>, 3<sup>T</sup>, 6<sup>T</sup>, and 9<sup>T</sup> using the HF-US imaging system (VEVO770 with a 25 MHz transducer), and their volume was calculated as described previously.<sup>7</sup> Mouse body weight was measured on days -7<sup>T</sup>, 0<sup>T</sup>, 3<sup>T</sup>, 6<sup>T</sup>, and 9<sup>T</sup>. As there were no statistically significant toxicity or blood biochemical parameter changes (T-Bil, ALT, AST, Cre, or BUN) in our previous study using CDDP at 5 mg/kg<sup>16</sup>, these parameters were not examined in the present study, when a concentration of CDDP of 1 mg/kg was investigated.

## 2.7 | Histological analysis

The SiLN and PALN were removed on day 0<sup>T</sup> (without drug injection) or 9<sup>T</sup>, immersed in 10% formalin solution for 4 days at room temperature, and dehydrated in 100% ethanol for 2 days at room temperature. The ethanol-exchanged organs were paraffin-embedded in a closed automated inclusion system (Shandon Excelsior ES™; Thermo Fisher Scientific), and 2.5- $\mu$ m sections were prepared. In addition to hematoxylin-eosin (HE) staining, lymphatic endothelial cells were immunohistochemically stained with rabbit anti-LYVE-1 antibody (1:250; 103-PA50AG; ReliaTech). Images were acquired with a BX51 polarized light microscope equipped with a DP21 digital camera (Olympus).

## 2.8 | Statistical analysis

Prism 8 (GraphPad Software) was used for all statistical analyses. Data are expressed as the mean  $\pm$  standard error of the mean (mean  $\pm$  SEM). Two-way ANOVA, Tukey's multiple comparison test, Šidák's multiple comparison test, and a paired *t* test were used to look for significant differences.  $P < .05$  was considered to be statistically significant.

### 3 | RESULTS

#### 3.1 | Pathological changes in metastatic LNs

In this study, we first inoculated tumor cells into the PALN and then injected solution with/without CDDP into the SILN 7 days later to deliver the solution to the PALN. As the LDDS was developed to target LNs in the early stage of metastasis, initially we investigated whether the inoculated LN was at a stage of tumor

development that was similar to that seen in early-stage metastasis. Figure 1 shows images of the PALN on day 7 after tumor cell inoculation. Comparisons of serial sections revealed that tumor cells had proliferated in the LN to fill and obstruct the lymphatic sinuses (Figure 1Ai). In some regions, the lymphatic endothelium had been lost, and tumor cells had extended beyond the lymph sinusoids to infiltrate the surrounding tissue (Figure 1Aii). Three-dimensional HF-US imaging (Figure 1B,C) did not show any PALN volume changes between day 0 (day  $-7^T$ , just before tumor cell inoculation) and day

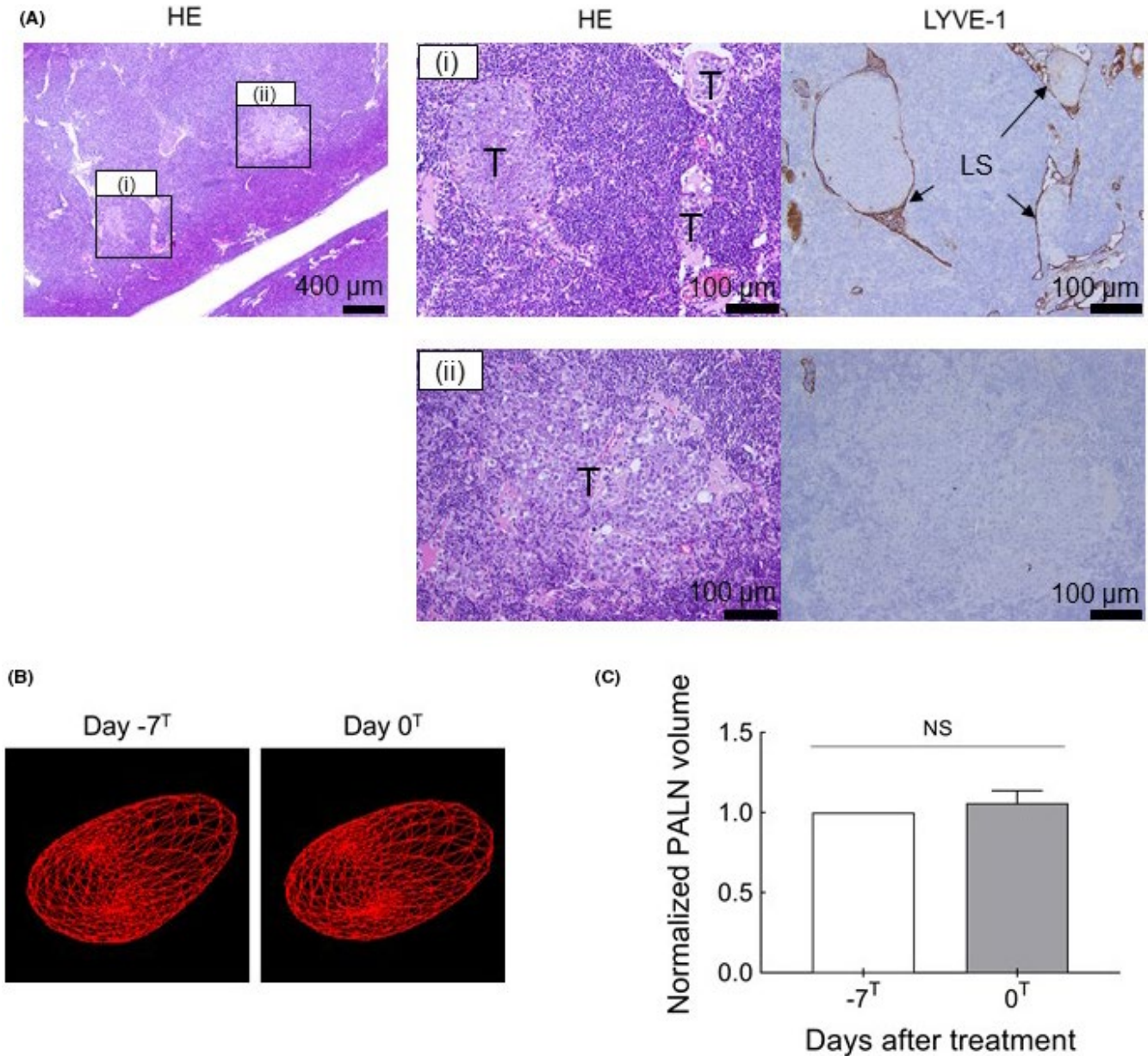


**FIGURE 1** Histopathological images of the proper axillary lymph node (PALN) immediately before the therapeutic intervention. A, The HE-stained and LYVE-1-immunostained sections on the right correspond to regions (i) and (ii) in the HE-stained section on the left. (i) Tumor infiltration and growth were observed in the lymph node (LN). Tumor cells had grown along the lymphatics to fill the lymphatic sinuses as tumor emboli. Furthermore, the proliferating tumor had destroyed the structure of the lymphatic sinus and infiltrated the LN parenchyma. (ii) LYVE-1-positive cells were not detected, indicating destruction of the lymphatic sinus endothelium. LS, lymphatic sinus; T, tumor cells. Scale bars: 400  $\mu\text{m}$  and 100  $\mu\text{m}$ . B, Three-dimensional reconstruction of the high-frequency ultrasound system (HF-US) imaging data for the PALN at day  $-7^T$  and day  $0^T$ . The segmented LN borders are shown in red. C, PALN volume normalized to the value at day  $-7^T$ . There was no significant difference in PALN volume between days  $-7^T$  and  $0^T$  (paired *t* test). Data are presented as mean  $\pm$  SEM (*n* = 6). NS: not significant

7 (day 0<sup>T</sup>, just before treatment). Therefore, the pathological status of the PALN was comparable to that seen in early-stage metastasis (ie, the PALN corresponded to a “false-negative” LN in which metastasis would not be detected by imaging modalities presently used in clinical practice).

### 3.2 | Intranodal lymphangiography of the PALN using contrast-enhanced HF-US imaging

As a first step to investigating the optimal osmotic pressure and viscosity of the drug solvent, we evaluated the delivery of two Sonazoid-containing solutions (solution I and II) from the SiLN to the tumor-containing PALN (Figure 2). In experiments in which the SiLN was injected with solution I, which had the same osmotic pressure and viscosity as saline (II: 588 kPa;  $\mu$ : 1 mPa-s), the marginal sinus of the PALN showed strong contrast enhancement, whereas

the lymphatic sinuses in the PALN showed weak contrast enhancement (Figure 2A). On the other hand, following the injection of solution II, which had the same viscosity as saline but a higher osmotic pressure (II: 3,000 kPa,  $\mu$ : 1 mPa-s), both the marginal sinuses and lymphatic sinuses of the PALN showed strong enhancement, which increased with time (Figure 2A). The volume of the PALN (normalized to the value before injection) tended to increase with time during the first 12 minutes after the injection of solution II (Figure 2B). However, there was no significant difference in the change in PALN volume between solutions I and II (two-way ANOVA and Šidák's multiple comparison test). Figure 2C shows temporal changes in the proportion of the PALN showing contrast enhancement after the injection of contrast medium in solution I or II. The proportion of the PALN showing contrast enhancement increased to reach a peak value of ~ 10% at 12 minutes after starting the injection of solution I and ~ 40% at 20 minutes after starting the injection of solution II. Notably, the proportion of the PALN showing contrast enhancement

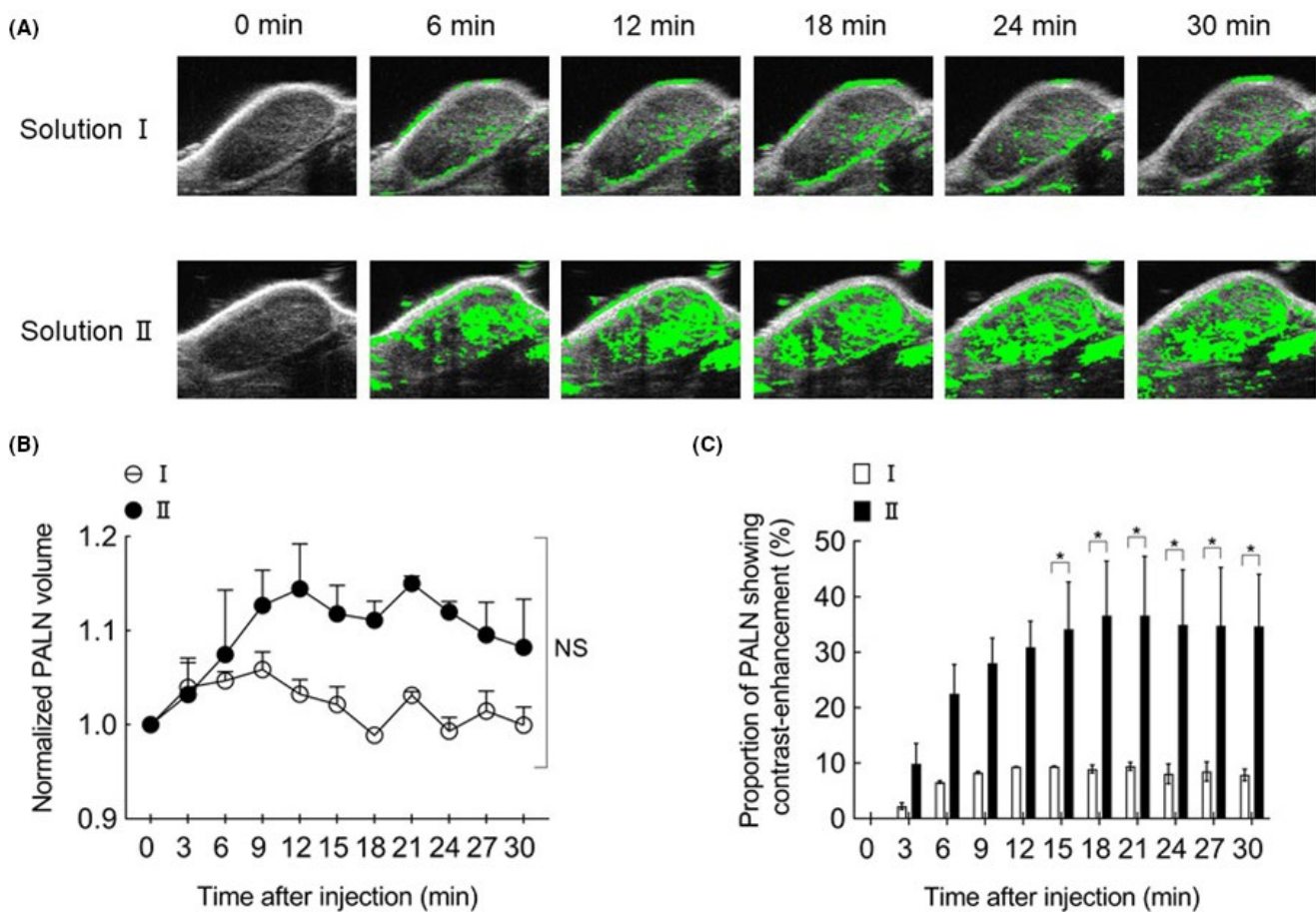


**FIGURE 2** Intranodal lymphangiography of the proper axillary lymph node (PALN) using contrast-enhanced high-frequency ultrasound system (HF-US) imaging. A, Intranodal lymphangiography. Regions in which the change in brightness value exceeded a certain threshold relative to the image before the injection of ultrasound contrast medium (0 min) are indicated in green. The lymphatic sinuses of the PALN were dilated following the administration of solution II. B, Changes in PALN volume following the infusion of solutions with different osmolarities. PALN volume (normalized to the value at 0 min) after the administration of solution I did not differ significantly between solution I and solution II. NS: not significant. C, Temporal changes in the proportion of the PALN showing contrast enhancement after the injection of ultrasound contrast medium in solution I or II. There was a significant difference between groups in the proportion of the PALN showing contrast enhancement at 15-30 min after the injection (two-way ANOVA and Šidák's multiple comparison test: \**P* < .05, solution I vs solution II). Data are presented as mean  $\pm$  SEM (*n* = 2)

differed significantly between the two solutions at 15–30 minutes ( $P < .05$ ).

In subsequent experiments, the SiLN was injected on day 7 ( $0^T$ ) with CDDP dissolved in solution III, IV, or V (all of which contained ICG) to treat the tumor cell-inoculated PALN. Fluorescence imaging (Figure 3) revealed that the injected solution flowed from the SiLN to the PALN and in all cases was retained in the SiLN until day  $9^T$ . There were no significant differences between solutions III, IV, or V in the normalized fluorescence intensity in the SiLN after injection at day  $0^T$ , but solution V appeared to be better retained in the SiLN (Figure 3B). Solutions III and IV were retained in the PALN until day  $3^T$ , whereas solution V was partly retained until day  $9^T$  (Figure 3C). There were significant differences between solutions in the PALN fluorescence intensity at day  $0^T$ , with the highest level observed for solution III and the lowest level for solution V ( $P < .05$ ; Figure 3C).

These results suggest that the higher viscosity of solution V resulted in better retention in the SiLN and slower delivery to the PALN. Intravenous injection resulted in the rapid delivery of ICG to the whole body (particularly the liver), but there was no accumulation of ICG in the PALN (Figure 3A). The images did not allow us to compare the results of intravenous injection with those of the other groups because it was not possible to determine whether the intravenously injected solution had accumulated specifically in the PALN or SiLN rather than in overlying tissues.

Figure 4A shows the luciferase activity of tumor cells during the course of treatment. Strong luciferase activity was observed in the PALN after the administration of solutions III or IV with the LDDS or solution III(+CDDP) by intravenous injection. On the other hand, the administration of solution III(+CDDP), IV(+CDDP), or V(+CDDP) with the LDDS inhibited tumor growth,

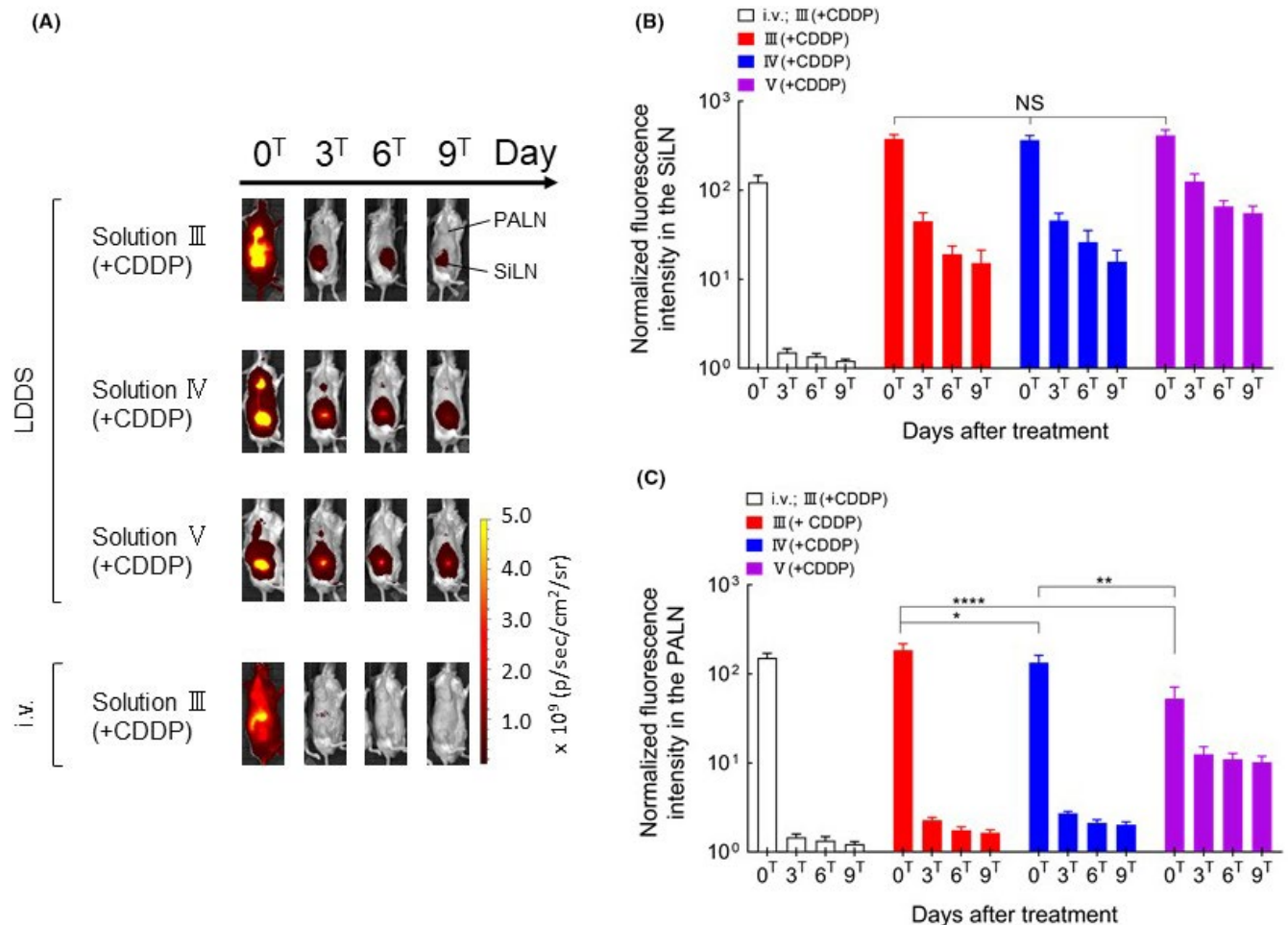


**FIGURE 3** Changes in fluorescence intensity over time after the administration of indocyanine green (ICG) using the lymphatic drug delivery system (LDDS). A, Representative images showing ICG fluorescence intensity. B, Temporal changes in ICG fluorescence intensity in the subiliac LN (SiLN). There were no significant differences in ICG fluorescence intensity in the SiLN between the solution groups for all time points. C, Temporal changes in ICG fluorescence intensity in the proper axillary lymph node (PALN). ICG fluorescence intensity at days  $0^T$ ,  $3^T$ ,  $6^T$ , and  $9^T$  were normalized to the value before injection. There were no statistically significant differences in ICG fluorescence intensity between the III(+CDDP), IV(+CDDP), and V(+CDDP) groups at day  $3^T$ ,  $6^T$ , and  $9^T$ . ICG fluorescence intensity at day  $0^T$  differed significantly between the III(+CDDP), IV(+CDDP) and V(+CDDP) groups (\*\*\*\*,  $P < .0001$ , III(+CDDP) vs V(+CDDP); \*\* $P < .01$ , IV(+CDDP) vs V(+CDDP); \* $P < .05$ , III(+CDDP) vs IV(+CDDP)). Data are presented as the mean  $\pm$  SEM (i.v. III(+CDDP),  $n = 6$ ; III(+CDDP),  $n = 7$ ; IV(+CDDP),  $n = 6$ ; V(+CDDP),  $n = 4$ )

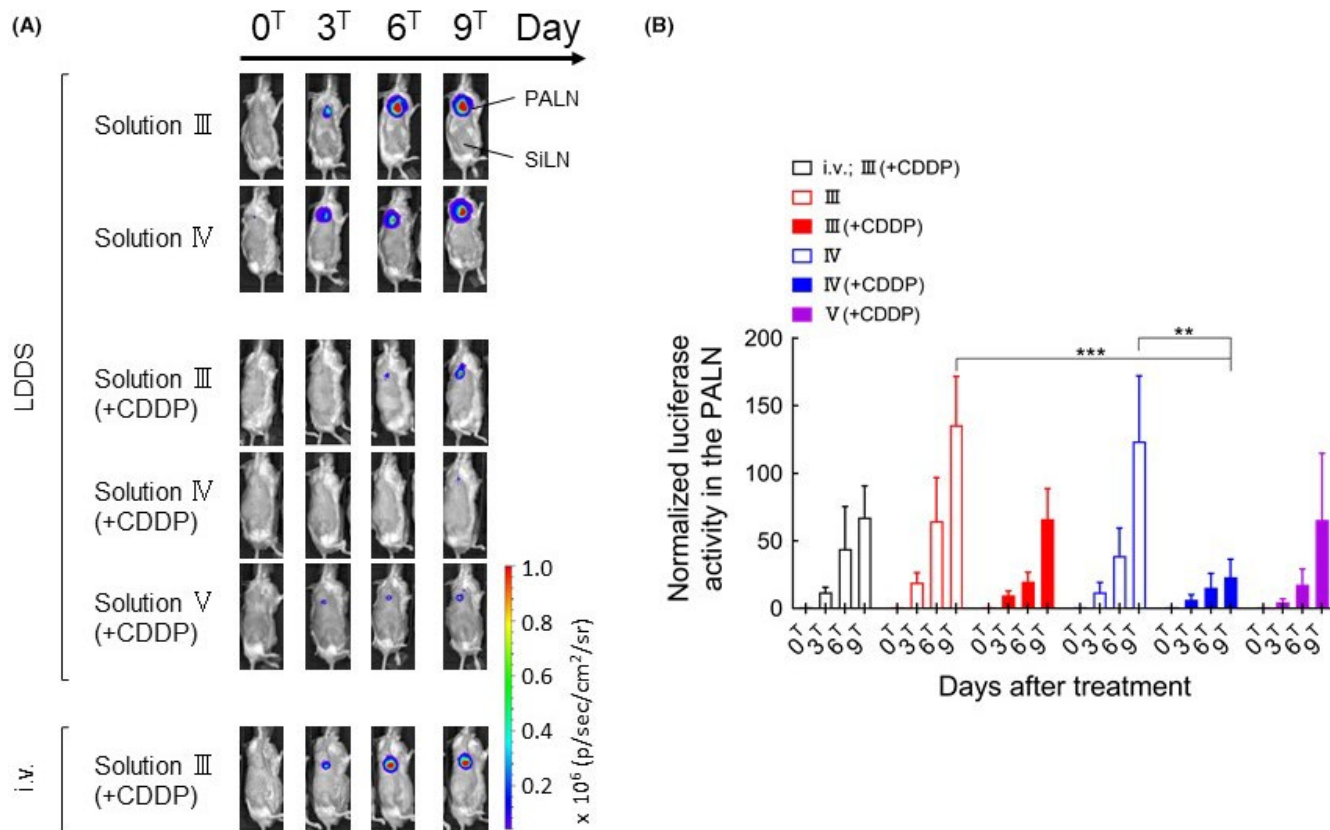


**FIGURE 4** Changes in bioluminescence intensity over time after the administration of cisplatin (CDDP) using the lymphatic drug delivery system (LDDS). A, Representative bioluminescence images showing luciferase activity. B, Luciferase activity in the proper axillary lymph node (PALN) normalized to the value at day 0<sup>T</sup>. Bioluminescence intensity at day 9<sup>T</sup> was significantly lower in the IV(+CDDP) group than in the III or IV groups (two-way ANOVA and Tukey's test: \*\*\* $P < .001$ , III vs IV(+CDDP); \*\* $P < .01$ , IV vs IV(+CDDP)). There were no statistically significant differences in the bioluminescence intensity among III(+CDDP), IV(+CDDP), and V(+CDDP) at day 9<sup>T</sup>. Data are presented as the mean  $\pm$  SEM (i.v. III(+CDDP),  $n = 6$ ; III,  $n = 6$ ; III(+CDDP),  $n = 7$ ; IV,  $n = 6$ ; IV(+CDDP),  $n = 6$ ; V(+CDDP),  $n = 4$ )

and the inhibition of tumor growth by IV(+CDDP) was particularly pronounced at day 9<sup>T</sup> ( $P < .001$ , III vs IV(+CDDP);  $P < .01$ , IV vs IV(+CDDP); Figure 4B).

HF-US images showing the maximal cross-sections and calculated volumes of the SiLN and PALN are presented in Figure 5. No morphological changes were observed around the SiLN at the site of drug injection after the administration of solution III(+CDDP) by the LDDS, but edema (yellow arrows) was observed around the SiLN until day 6<sup>T</sup> after the administration of solution IV(+CDDP) and day 9<sup>T</sup> after the administration of solution V(+CDDP). By contrast, no clear edematous changes were observed in the PALN in any of the groups. SiLN volume decreased after the administration of CDDP-containing solutions with the LDDS, and a similar but smaller trend was observed for PALN volume. However, intravenous injection of solution III(+CDDP) was associated with little or no change in PALN volume over time and a tendency toward a slight increase in SiLN volume, which was likely due to the lymphadenopathy inherent in MXH10/Mo/lpr mice. Histological observations of the SiLN (Figure S1) showed that the original structure of the LN was maintained after the administration of solution III, whereas the lymphatic sinus was dilated following the administration of solution IV. Necrosis in the SiLN was observed in the

III(+CDDP), IV(+CDDP), and V(+CDDP) groups. Observation of the PALN revealed the presence of tumor cells in the lymphatic sinus and parenchyma after the administration of solution III(+CDDP) or V(+CDDP), whereas only a few tumor cells remained in the lymphatic sinus and parenchyma after the administration of solution IV(+CDDP). Tumor growth was observed after intravenous injection of solution III(+CDDP) (Figure 6). There were no significant differences in body weight between the various groups (Figure S2). The above findings indicate that tumor growth was inhibited most by solution IV(+CDDP).

## 4 | DISCUSSION

In this study, the SiLN was used as a model of an upstream normal LN and the PALN was used as a model of a downstream LN (SLN) in the early stage of metastasis. CDDP solution was injected into the SiLN by the LDDS so that it would be delivered to the PALN, and the values of the osmotic pressure and viscosity of the solvent that maximized the antitumor effects of CDDP were determined. Solution IV (II: 1897 kPa;  $\mu$ : 12 mPa·s) was found to have remarkable potential for the suppression of

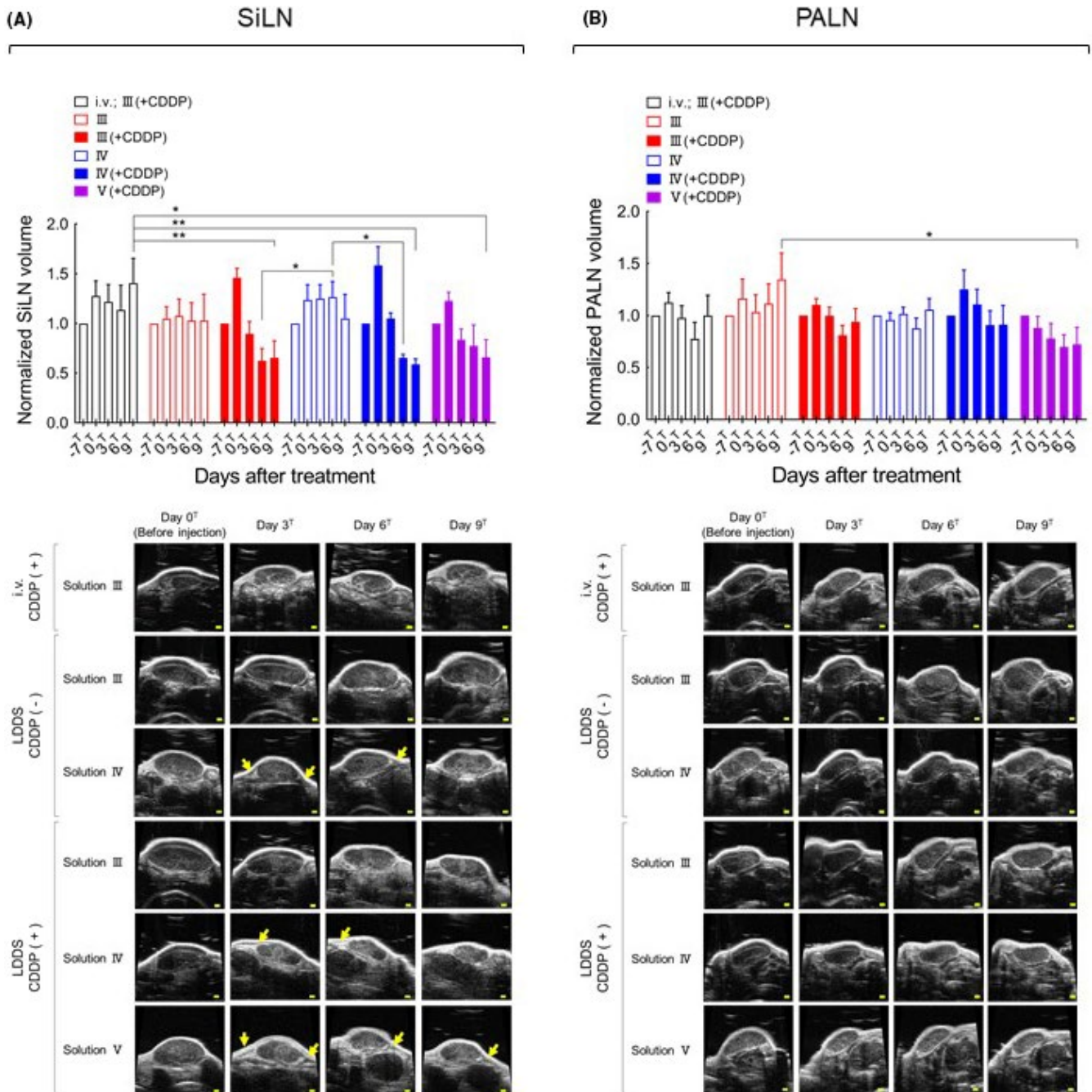


**FIGURE 5** Changes in subiliac lymph node (SiLN) and proper axillary lymph node (PALN) volumes after cisplatin (CDDP) administration using the lymphatic drug delivery system (LDDS). A, SiLN volume normalized to the value at day  $-7^T$ . SiLN volume at day  $6^T$  was significantly smaller in the III(+CDDP) and IV(+CDDP) groups than in the IV group (two-way ANOVA and Tukey's test:  $*P < .05$ , III[+CDDP] vs IV; IV vs IV[+CDDP]). SiLN volume at day  $9^T$  was significantly smaller in the III(+CDDP), IV(+CDDP), and V(+CDDP) groups than in the i.v. III(+CDDP) group (two-way ANOVA and Tukey's test:  $**P < .01$ , i.v. III[+CDDP] vs III[+CDDP], i.v. III[+CDDP] vs IV[+CDDP];  $*P < .05$ , i.v. III[+CDDP] vs V[+CDDP]). The B-mode ultrasound images show the maximal plane of the lymph node (LN). Edematous changes are indicated by yellow arrows. Scale bars: 1 mm. B, PALN volume normalized to the value at day  $-7^T$ . PALN volume at day  $9^T$  was significantly smaller in the V(+CDDP) group than in the III group (two-way ANOVA and Tukey's test:  $*P < .05$ , III vs V[+CDDP]). Data are presented as the mean  $\pm$  SEM (i.v. III[+CDDP],  $n = 6$ ; III,  $n = 6$ ; III[+CDDP],  $n = 7$ ; IV,  $n = 6$ ; IV[+CDDP],  $n = 6$ ; V[+CDDP],  $n = 4$ ). The B-mode ultrasound images show the maximal plane of the LN. Scale bars: 1 mm

tumor growth in the PALN. Delivery of a solution with high osmotic pressure resulted in dilation of the lymphatic sinuses in the PALN. When solution II was used, expansion of the lymphatic

sinuses in the PALN reached a maximum at 21 minutes and was maintained thereafter (Figure 2C). We suggest that the dilation of the lymphatic sinuses occurs due to the flow of fluid into the

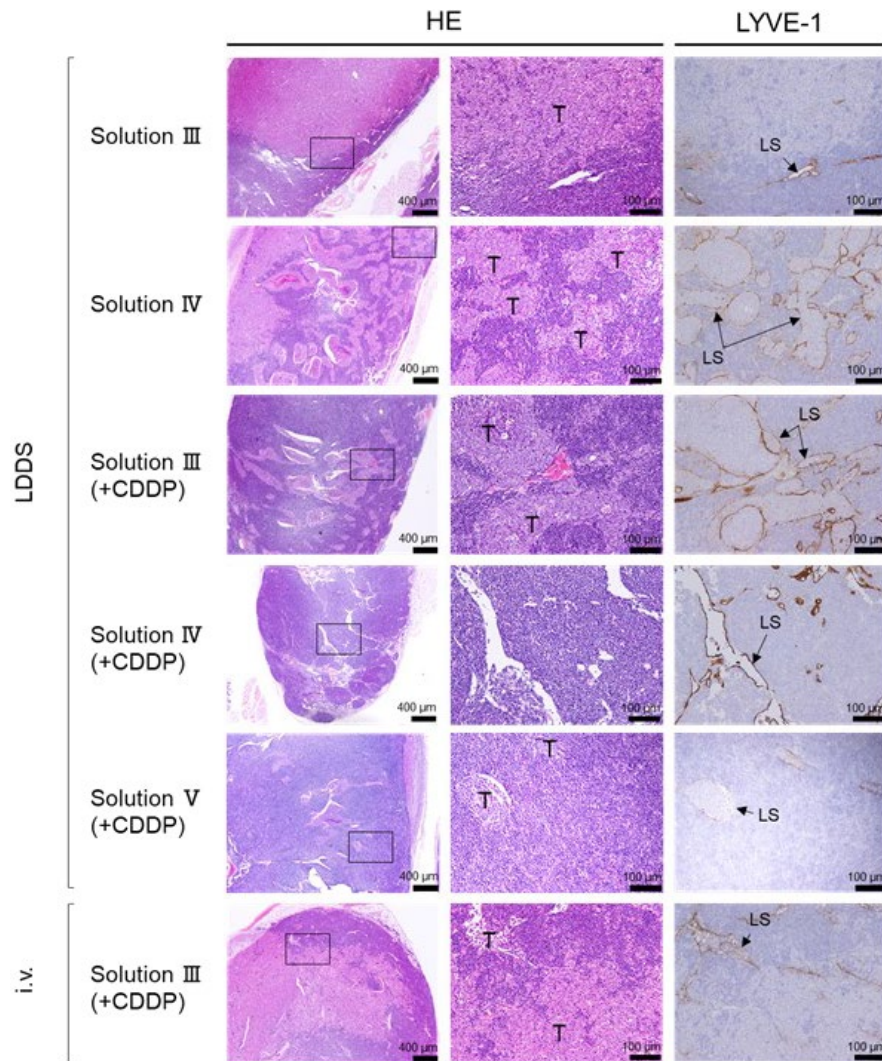


**FIGURE 6** Histopathological changes in the proper axillary lymph node (PALN) after cisplatin (CDDP) administration into SiLN using the lymphatic drug delivery system (LDDS). The HE-stained and LYVE-1-immunostained sections on the right correspond to the regions indicated by rectangles in the HE-stained sections on the left. Solution III administered using the LDDS: Tumor cells had infiltrated the lymph node (LN) parenchyma and destroyed the normal structure of the lymphatic sinuses, and LYVE-1-positive lymphatic sinus endothelial cells were absent from the tumor-infiltrated area. Solution IV administered using the LDDS: Tumor cells had grown along and filled the lymphatic sinus as tumor emboli. Solution III(+CDDP) administered using the LDDS: Tumor cells had proliferated along the lymphatic sinus to fill it as tumor emboli; an antitumor effect of CDDP could not be confirmed. Solution IV(+CDDP) administered using the LDDS: The lymphatic sinuses were dilated, but no tumor cells were identified. Solution V(+CDDP) administered using the LDDS: The lymphatic sinuses were dilated, and residual tumor cells were found in the sinuses and LN parenchyma. Solution III(+CDDP) administered intravenously: Tumor cells had infiltrated the LN parenchyma and destroyed the structure of the lymphatic sinuses; LYVE-1-positive lymphatic sinus endothelial cells were absent at the site of tumor invasion. HE: hematoxylin-eosin staining; LS: lymphatic sinus; LYVE-1: immunohistochemical staining using anti-LYVE-1 antibody; T: tumor cells. Scale bars: 400  $\mu\text{m}$  and 100  $\mu\text{m}$

sinuses to reduce the osmotic pressure of the solvent, and we speculate that this fluid is derived from afferent lymphatic vessels, capillaries, postcapillary vessels (high endothelial venules), and/or the central region of the thoracoepigastric vein (which connects the SiLN and PALN), where blood flow occurs in two directions: one oriented toward the PALN and the other toward the SiLN.<sup>14</sup> Edematous changes were observed around the SiLN after the administration of solution IV or V (Figure 5A). When a solution with high osmotic pressure was injected into the SiLN, it tended to leak out of the LN, resulting in an accumulation of

interstitial fluid around the SiLN to reduce the osmotic pressure. These edematous changes were considered to be a mild adverse effect of injection because they were localized and differed from the severe edema associated with lymphatic system dysfunction after LN dissection. When CDDP-containing solutions III, IV, or V were administered, the volumes of the SiLN and PALN decreased, which may have been due to damage to the lymphocytes in these LNs. As intravenous injection of CDDP in solution III did not exert any antitumor effects, the osmotic pressure of saline may not be suitable for the effective treatment of metastatic

LN. Our experiments indicate that the optimal osmotic pressure of the solvent is higher than the osmotic pressure of saline and lower than 3,000 kPa. An increase in solvent viscosity enhanced the retention of the solution in the SiLN and induced necrosis (Figure S1). Increasing solvent viscosity also reduced the rate of delivery to the PALN (Figure 3), resulting in a smaller antitumor effect (Figure 4). CDDP administered intravenously or with the LDDS did not exert a clear antitumor effect when solution III was used, which has the same viscosity as saline. From the above, a solvent with an osmotic pressure and viscosity of 1,900 kPa and 12 mPa·s would be suitable for use in the LDDS. Osmotic pressure and viscosity are independent factors, so it will be important to determine the optimal ranges for both parameters and establish whether the optimal ranges vary between different types of anticancer drug.

### CONFLICT OF INTEREST

Tetsuya Kodama received commercial research support from Yakult Honsha Co., Ltd. The other authors declare no conflict of interest.

### AUTHOR CONTRIBUTIONS

RF conceived the hypothesis, conducted all the experiments, and analyzed most of the data. AS, RM, and MS interpreted the experimental data. SM designed and conducted the pathology experiments and interpreted the experimental data. TK conceived the hypothesis, interpreted all the experimental data, and supervised the project. All authors critically revised the manuscript and approved the final submitted version.

### ORCID

Ariunbuyan Sukhbaatar  <https://orcid.org/0000-0001-9137-2966>

Tetsuya Kodama  <https://orcid.org/0000-0003-4727-9558>

### REFERENCES

1. Tateda M, Shiga K, Yoshida H, et al. Management of the patients with hypopharyngeal cancer: eight-year experience of miyagi cancer center in Japan. *Tohoku J Exp Med*. 2005;205:65-77.
2. Shiga K, Ogawa T, Kobayashi T, et al. Malignant melanoma of the head and neck: a multi-institutional retrospective analysis of cases in northern Japan. *Head Neck*. 2012;34:1537-1541.
3. Kelch ID, Bogle G, Sands GB, Phillips AR, LeGrice IJ, Dunbar PR. Organ-wide 3D-imaging and topological analysis of the continuous microvascular network in a murine lymph node. *Sci Rep*. 2015;5:16534.
4. Kodama T, Mori S, Nose M. Tumor cell invasion from the marginal sinus into extranodal veins during early-stage lymph node metastasis can be a starting point for hematogenous metastasis. *J Cancer Metastasis Treat*. 2018;4:56.
5. Mikada M, Sukhbaatar A, Miura Y, et al. Evaluation of the enhanced permeability and retention effect in the early stages of lymph node metastasis. *Cancer Sci*. 2017;108:846-852.
6. Jeong HS, Jones D, Liao S, et al. Investigation of the lack of angiogenesis in the formation of lymph node metastases. *J Natl Cancer Inst*. 2015;107.
7. Fujii H, Horie S, Sukhbaatar A, et al. Treatment of false-negative metastatic lymph nodes by a lymphatic drug delivery system with 5-fluorouracil. *Cancer Med-U.S*. 2019;8:2241-2251.
8. Iwamura R, Sakamoto M, Mori S, Kodama T. Imaging of the mouse lymphatic sinus during early stage lymph node metastasis using intranodal lymphangiography with X-ray micro-computed tomography. *Mol Imaging Biol*. 2019;21:825-834.
9. Matsumura Y, Maeda H. A new concept for macromolecular therapeutics in cancer chemotherapy: mechanism of tumorotropic accumulation of proteins and the antitumor agent smancs. *Cancer Res*. 1986;46:6387-6392.
10. Leong SPL, Morita ET, Südmeyer M, et al. Heterogeneous patterns of lymphatic drainage to sentinel lymph nodes by primary melanoma from different anatomic sites. *Clin Nucl Med*. 2005;30:150-158.
11. Trevaskis NL, Kaminskas LM, Porter CJ. From sewer to saviour - targeting the lymphatic system to promote drug exposure and activity. *Nat Rev Drug Discov*. 2015;14:781-803.
12. Topalian SL, Taube JM, Pardoll DM. Neoadjuvant checkpoint blockade for cancer immunotherapy. *Science*. 2020;367.
13. Shao LA, Takeda K, Kato S, Mori S, Kodama T. Communication between lymphatic and venous systems in mice. *J Immunol Methods*. 2015;424:100-105.
14. Takeda K, Mori S, Kodama T. Study of fluid dynamics reveals direct communications between lymphatic vessels and venous blood vessels at lymph nodes of mice. *J Immunol Methods*. 2017;445:1-9.
15. Kodama T, Matsuki D, Tada A, Takeda K, Mori S. New concept for the prevention and treatment of metastatic lymph nodes using chemotherapy administered via the lymphatic network. *Sci Rep-Uk*. 2016;6.
16. Tada A, Horie S, Mori S, Kodama T. Therapeutic effect of cisplatin given with a lymphatic drug delivery system on false-negative metastatic lymph nodes. *Cancer Sci*. 2017;108:2115-2121.
17. Kodama T, Mori S. Optimized ranges of osmotic pressure and viscosity of drugs required for lymphatic drug delivery system. AACR Annual Meeting 2019. Atlanta, Georgia, USA, 2019.
18. Kawai M, Wray JS, Zhao Y. The effect of lattice spacing change on cross-bridge kinetics in chemically skinned rabbit psoas muscle fibers. I. Proportionality between the lattice spacing and the fiber width. *Biophys J*. 1993;64:187-196.
19. Shao L, Mori S, Yagishita Y, et al. Lymphatic mapping of mice with systemic lymphoproliferative disorder: usefulness as an inter-lymph node metastasis model of cancer. *J Immunol Methods*. 2013;389:69-78.
20. Miura Y, Mikada M, Ouchi T, et al. Early diagnosis of lymph node metastasis: importance of intranodal pressures. *Cancer Sci*. 2016;107:224-232.
21. Van den Broeck W, Derore A, Simoens P. Anatomy and nomenclature of murine lymph nodes: descriptive study and nomenclature standardization in BALB/cAnNCrI mice. *J Immunol Methods*. 2006;312:12-19.
22. Li L, Mori S, Kodama M, Sakamoto M, Takahashi S, Kodama T. Enhanced sonographic imaging to diagnose lymph node metastasis: importance of blood vessel volume and density. *Cancer Res*. 2013;73:2082-2092.
23. Li L, Mori S, Sakamoto M, Takahashi S, Kodama T. Mouse model of lymph node metastasis via afferent lymphatic vessels for development of imaging modalities. *PLoS One*. 2013;8:e55797.
24. Kato S, Shirai Y, Kanzaki H, Sakamoto M, Mori S, Kodama T. Delivery of molecules to the lymph node via lymphatic vessels using ultrasound and nano/microbubbles. *Ultrasound Med Biol*. 2015;41:1411-1421.
25. Kato S, Shirai Y, Motozono C, Kanzaki H, Mori S, Kodama T. In vivo delivery of an exogenous molecule into murine T lymphocytes using a lymphatic drug delivery system combined with sonoporation. *Biochem Biophys Res Commun*. 2020;525:1025-1031.

26. Fujii H, Horie S, Takeda K, Mori S, Kodama T. Optimal range of injection rates for a lymphatic drug delivery system. *J Biophotonics*. 2018;11:e201700401.

#### SUPPORTING INFORMATION

Additional supporting information may be found online in the Supporting Information section.

**How to cite this article:** Fukumura R, Sukhbaatar A, Mishra R, Sakamoto M, Mori S, Kodama T. Study of the physicochemical properties of drugs suitable for administration using a lymphatic drug delivery system. *Cancer Sci*. 2021;112:1735-1745. <https://doi.org/10.1111/cas.14867>